SIMULATING SEISMIC WAVE PROPAGATION IN TRANSVERSELY ISOTROPIC MEDIA BY USING PSEUDO-SPECTRAL METHOD

ZHANG Fan-min[1], Takenaka Hiroshi[2], Li Qing-he[1], WANG Yan-bin[2]
(1. *Lanzhou Institute of Seismology, CSB, Lanzhou* 730000, *China*;
2. *Dept. of Earth & Planetary Sciences, Faculty of Science, Kyushu Univ., Fukuoka* 812-81, *Japan*)

Abstract

The elastic constant is a component of a three-dimensional fourth-rank tensor, having 81 components, in all. According to the symmetry of both the stress and strain tensors and the existence of a density energy function, which is quadratic in strain, the number of independent constants is 21 for general anisotropic media. The number of independent elastic constants can be reduced still mord if media have higher symmetry. Transversely isotropic medium, which has only five indepindent constants, is a good approximation of rocks in the crust and the upper mantle of the earth. In this paper, we are concerned about transversely isotropic media with an arbitrary direction of symmetrical axis(i.e., the symmetrical axis may not be parallel to the verticalaxis). In this case we need to change coordinates from one system to another. If we know the elastic constants in one particular coordinate system, for example, whose axes are parallel or perpendicular to the symmetrical axis of the midia, we can easily obtain these elastic constants in new coordinate system by using the transformation formula.

In this paper we present an approach for modeling wave-fields excited by not only a source but also a plane-wave incidence in transversely isotropic media mentioned above by the pseudo-spectral method. Modeling of planc waves propagating in transversely isotropic media is one of the most important subjects as well as that of waves emitted from a localized source in exploration geophsics and seismology. While it is deffcult or even impossible to determine the phase velocity and the polarization direction of plane waves in general anisotropic media, in the case of transversely isotropic media we can achieve this purpose through coordinate transformation. We here develop a scheme that can be used for plane-wave modeling in travsversely isotropic media.

Key words: Numerical simulation; Seismic wave; Anisotropy; Transversely isotropy; Pseudo-spectral method

0 Introduction

In the last three decades, seismologists and geophysicists have obtained much seismological evidence, which shows that the media of the crust and the upper mantle are inhomogeneous and anisotropic[1~3]. Recent studies indicate that the inner core also displays transversely isotropic properties[4~5]. So anisotropy may be a universal phenomenon in the earth. In the crust and the upper mantle, anisotropy usually results from the physics properties of crystalline solids or minerals such as olivine and pyroxene, whose lattice have preferred orientations, or is caused by finely layered media or by the stress-aligned micro-cracks which are usually filled with water[3,6]. Transversely isotropic medium is a good approximation of such media[7~8]. However, the cause of anisotropy in the inner core has not been clearly known yet[4~5]. So the knowledge on anisotropic media, particularly on transversely isotropic media, is very important for us to understand the properties of seismic waves propagating in the earth and to get the deep structure information carried by these waves. Unfortunately, the wave equations in inhomogeneous anisotropic media are very complicated because three displacement components are coupled together. It is difficult or impossible to obtain analytical solutions of these equations. However, with the development of computer techniques, to some extent, it has become possible to get numerical solutions on high performance work stations or on super computers, even for a three dimensional anisotropic model[9~13]. Synthetic seismograms and snapshots can help us understand wave propagation and wave field variation in detail in a given model, thus bringing us potentials to learn real media of the earth.

There are several methods which have already been developed to calculate synthetic seismograms and seismic wave propagation in anisotropic media, such as reflectivity method which is only for layered laterally homogeneous anisotropic media and asymptom ray theory which only can be used for the media with weak anisotropy and fail to calculate seismograms accurately for the media with large velocity variations[14]. Numerical solution methods such as the finite difference method and finite element method[18] have also been used to calculate seismic waves in heterogeneous media. However, these methods are limited by their disadvatages. In order to obtain relatively accurate results, we have to discretize mode into, at least, 10 grid points per wavelength if we use second-order finite differencing. So, for 3-D model or anisotropic model which has 21 elastic constants, it is difficult to use finite difference method (FDM) or finite element method (FEM) to obtain satisfying results, even on a large super computer. Another numerical method, the pseudo-spectral method(PSM), has already been used widely in seismology to simulate wave field because of its high efficiency[19~23]. Fornberg (1987) shows that the PSM requires, in each spatial dimension, as few as a quarter of the number of grid points of fourth-order finite differencing, and one-sixteenth the number of points of second-order finite differencing and can be expected to run about 150 times faster and use less the 1/2000 of the memory required by the secondorder finite difference method. The pseudo-spectral method can be regarded as an alternative to the finite difference method and finite element method[21~24]. In this study, we use psudo-spectral method to simulate seismic wave field in transversely isotropic heterogeneous media with arbitrary directions of symmetrical axes.

1 Wave Equations in General Anisotropic Media

The equations of motion for seismic waves in elastic, inhomogeneous anisotropic media can be written as

$$\rho \ddot{U}_i = \frac{\partial}{\partial x_j}(c_{ijkl}\varepsilon_{kl}) + f_i \tag{1}$$

where c_{ijkl} are elastic constants and ε_{kl} are strain tensor which is written as

$$\varepsilon_{kl} = \frac{1}{2}\left(\frac{\partial U_l}{\partial x_k} + \frac{\partial U_k}{\partial x_l}\right) \tag{2}$$

where x_i is a Cartesian coordinate corresponding to x, y and z, U_i is the displacement in the x_i direction, and c_{ijkl} is a component of a three dimensional fourth-rank tensor, having 81 components, in all. According to the symmetry of both the stress and strain tensors and the existence of density energy function that is quadratic in strain, we can write

$$c_{ijkl} = c_{jikl} = c_{ijlk} = c_{klij} \tag{3}$$

This symmetry condition means that there are 21 independent elastic constants for arbitrarily anisotropic media.

Sometimes, we need to change coordinates from one system to another. If we know the elastic constants in one particular coordinate system, for example, whose axes are parallel or perpendicular to the symmetrical axis of the media, we can easily obtain these elastic constants in a new coordinate system by using the following transformation formula:

$$c'_{ijkl} = \alpha_{ip}\alpha_{jq}\alpha_{kr}\alpha_{ls}c_{pqrs} \tag{4}$$

where c_{ijkl} are elastic constants in the new coordinate system, and α_{ij} are the elements of the transformation matrix from the old coordinate system to the new one.

2 Elastic Constants in Transversely Isotropic Media

From symmetrical conditions $c_{ijkl} = c_{jikl}$ and $c_{ijkl} = c_{ijlk}$, it is often convenient to describe anisotropic media by using 6×6 matrix C_{ij} instead of the full c_{ijkl} tensor components, Matrix C_{ij} can be defined

$$[C_{ij}] = \begin{bmatrix} c_{1111} & c_{1122} & c_{1133} & c_{1123} & c_{1113} & c_{1112} \\ c_{2211} & c_{2222} & c_{2233} & c_{2223} & c_{2213} & c_{2212} \\ c_{3311} & c_{3322} & c_{3333} & c_{3323} & c_{3313} & c_{3312} \\ c_{2311} & c_{2322} & c_{2333} & c_{2323} & c_{2313} & c_{2312} \\ c_{1311} & c_{1322} & c_{1333} & c_{1323} & c_{1313} & c_{1312} \\ c_{1211} & c_{1222} & c_{1233} & c_{1223} & c_{1213} & c_{1212} \end{bmatrix} \tag{5}$$

This is a symmetrical matrix because of the symmetry condition $c_{ijkl} = c_{klij}$ which means that the number of independent elastic constants for general anisotropic media is reduced to 21. The number of independent constants can be reduced still more if the media have higher symmetry. Transversely isotropic medium, which has only five independent constants because of higher symmetry, is a good approximation of rocks in the crust and the upper mantle of the earth[7~8]. In this paper, we are mainly concerned about such media.

For transversely isotropic media, if z-axis is parallel to the symmetrical axis of the media, C_{ij} can be weitten as following

$$[C_{ij}] = \begin{bmatrix} A & A-2N & F & 0 & 0 & 0 \\ F & A & F & 0 & 0 & 0 \\ F & F & C & 0 & 0 & 0 \\ 0 & 0 & 0 & L & 0 & 0 \\ 0 & 0 & 0 & 0 & L & 0 \\ 0 & 0 & 0 & 0 & 0 & N \end{bmatrix} \tag{6}$$

where= $A = c_{1111}$, $A - 2N = c_{1122}$, $F = c_{3333}$, $L = c_{1313}$ and $N = c_{1212}$.

3 Pseudo-spectral Method

Let U_i^n (l, m) and ρ(l, m) represent the displacement components and density at spatial grid point (l, m), and at the time step n. The spatial derivatives in equation (1) can be calculated by using the fast Fourier transform (FFT), and the time derivatives are approximated by differencing. Our method is similar to that of Reshefet al. (1988b). In this study, we use real FFT because of its calculation dfficiency and speed[12]. We can obtain the acceleration by using equation (4) and the wave field in the next time step is calculated by using following equations.

$$\dot{U}_i^{n+1/2} = \dot{U}_i^{n-1/2} + \Delta t \cdot \ddot{U}_i^n \tag{7}$$

$$U_i^{n+1} = U_i^n + \Delta t \cdot \dot{U}_i^{n+1/2} \tag{8}$$

where Δt is the time step which is selected small enouhg to keep the dispersion down to an acceptable level. Here, the criterion of Daudt et al. (1989), having following from, is used.

$$\Delta t < 0.26 \frac{\mathrm{Max}(\Delta x, \Delta y, \Delta z)}{V_P^{\max}} \tag{9}$$

where $V_P^{\max}$ is the maximum P-velocity in the model, and Max$(\Delta x, \Delta y, \Delta z)$ is the largest grid spacing[25].

4 Absorbing Boundary Conditions and Source Function

The weighting function for wave displacement is usually taken the following form[26]:

$$W(x, y, z) = \begin{cases} \exp[-k(x-b)^2] & \text{for } x < b \quad \text{or } x > L_x - b; \\ \exp[-k(y-b)^2] & \text{for } y < b \quad \text{or } y > L_y - b; \\ \exp[-k(z-b)^2] & \text{for } z < b \quad \text{or } z > L_z - b; \\ 1 \text{ elsewhere,} \end{cases} \tag{10}$$

where k is the absorption coefficient that is taken as 0.015 in this paper, b the width of tapered zone, and L_x, L_y, L_z are the model size in the x, y, and z direction, respectively.

The source function we used is a band-limited Ricker wavelet as follows

$$F(x, y, z) = [1 - 2\pi^2 f^2 (t - t_0)^2] \exp[-\pi^2 f^2 (t - t_0)^2] \cdot \exp\{[-\alpha(x - x_0)^2 + (y - y_0)^2 + (z - z_0)^2]\} \tag{11}$$

where x_0, y_0, z_0 is central position of the source, α determines the concentration of the source frnction, t_0 is the original time of the source function and f is the dominant frequency. This function can be directly used as a component of force (for instance, f_x) of a potential function of a pressure source or a shear source, from which we can calculate three components of the force, over a small region of the grid[20].

5 Formulations for Plane Waves in Transversely Isotropidc Media

When earthquakes occur very far from the receiver, the seismic waves can often be regarded as plane waves. Thus, to simulate plane waves propagating in transversely isotropic media is also very important in seismology. In general, it is deffcult or even impossible to determine the phase velocity and the polarization direction of plane waves in anisotropic media. But in the case of transversely isotropic media, we can achieve this purpose through coordinate transform. Here, we develop a method that can be used for plane wave modeling in transversely isotropic media.

If $\vec{u}(\vec{r},t)$ denotes the motion of a particle located at coordinates $\vec{r}$ at time t, the plane waves propagating in the direction $\vec{n}$ at phase velocity v can be written as:

$$\vec{u}(\vec{r},t) = \vec{a} f(\vec{n}\cdot\vec{r} - vt) \tag{12}$$

where $f(x)$ is an arbitrary function, $\vec{a}$ defines the amplitude and the polarization direction of the waves and $\vec{n}$ is a unit vector perpendicular to the phase surface.

If z-axis coincidences with the symmetrical axis of transversely isotropic media, while x-axis and y-axis can be set arbitrarily, velocities and polarization vectors for three types of waves can be written as[27]

$$\vec{a}_1 = \frac{\vec{e}\times\vec{n}}{|\vec{e}\times\vec{n}|} = \frac{\vec{e}\times\vec{n}}{\sqrt{1-(\vec{e}\cdot\vec{n})^2}} \tag{13}$$

$$\nu_1^2 = c_0 + c_3 \tag{14}$$

$$\vec{a}_2 = \vec{n} - \frac{c_1 - c_2 + \sqrt{(c_1-c_2)^2 + 4c_1c_2n_3^2}}{2c_1n_3}\vec{e} \tag{15}$$

$$\nu_2^2 = c_0 + \frac{1}{2}[c_1 + c_2 - \sqrt{(c_1-c_2)^2 + 4c_1c_2n_3^2}] \tag{16}$$

$$\vec{a}_0 = \vec{n} - \frac{c_1 - c_2 - \sqrt{(c_1-c_2)^2 + 4c_1c_2n_3^2}}{2c_1n_3}\vec{e} \tag{17}$$

$$\nu_0^2 = c_0 + \frac{1}{2}[c_1 + c_2 + \sqrt{(c_1-c_2)^2 + 4c_1c_2n_3^2}] \tag{18}$$

where $\vec{e}$ is a unit vector which denotes the direction of symmetrical axis of the media, c_0, c_1, c_2 and c_3 are constants, having following forms

$$\begin{aligned} c_0 &= g_1 + g_2n_3^2 \\ c_1 &= g_3 \\ c_2 &= g_2 + g_4n_3^2 \\ c_3 &= g_5(1-n_3^2) \end{aligned} \tag{19}$$

where n_3 is the directional cosine of the wave phase normal vector to z-axis in the old system, and

$$\left.\begin{aligned} g_1 &= \lambda_{1111} - \lambda_{1133} - \lambda_{2323} \\ g_2 &= 2\lambda_{2323} + \lambda_{1133} - \lambda_{1111} \\ g_3 &= \lambda_{1133} + \lambda_{2323} \\ g_4 &= \lambda_{1111} + \lambda_{3333} - 2\lambda_{1133} - 4\lambda_{2323} \\ g_5 &= \lambda_{1133} + \lambda_{2323} + \lambda_{1212} - \lambda_{1111} \end{aligned}\right\} \tag{20}$$

where $\lambda_{ijkl} = c_{ijkl}/\rho$. In geophysics and seismology, we take a coordinate system whose x-axis points to the north, y-axis to the east and z-axis down. The axis of the coordinate system is often not in the direction of the symmetrical axis of media. So in the seismic simulation, we have to rotate coordinate system. First, let coordinate system rotates an angle ψ around y-axis, then an angle ψ around z-axis. The transformation matrix can be written as

$$A = \begin{bmatrix} \cos(\varphi)\cos(\psi) & -\cos(\varphi)\sin(\psi) & \sin\varphi \\ \sin(\psi) & \cos(\psi) & 0 \\ -\sin(\varphi)\cos(\psi) & \sin(\varphi)\sin(\psi) & \cos(\varphi) \end{bmatrix} \tag{21}$$

In the new system, we assume that the phase normal has the following form

$$\vec{n} = [\sin(\theta) \quad 0 \quad \cos(\theta)]^T \tag{22}$$

By using (22), we can get phase normal corresponding to the old system as

$$\vec{n} = A^T\vec{n}' = \begin{bmatrix} n_1 \\ n_2 \\ n_3 \end{bmatrix} = \begin{bmatrix} \cos(\varphi)\cos(\psi)\sin(\theta) + \sin(\varphi)\cos(\theta) \\ \sin(\psi)\sin(\theta) \\ -\sin(\varphi)\cos(\psi)\sin(\theta) + \cos(\varphi)\cos(\theta) \end{bmatrix} \tag{23}$$

We can obtain the velocity of three types of plane waves by substituting (23) into (14), (16) and (18). In the old system, the symmetrical axis is parallel to the z-axis, which means

$$\vec{e} = [0 \quad 0 \quad 1]^T \tag{24}$$

Substituting (23) and (24) into (13), (15), and (17) and using the following equation

$$\vec{a}' = A\vec{a}' \tag{25}$$

we can obtain the polarization vectors for three types of waves in the new coordinate system.

6　Models and Calculation Results

In this paper, we calculated two 2-D models with the x-z section plane (Fig. 1). The positive directions of x-axis and z-axis point right and down, respectively. These models are composed of one layer and a half space and discretized into 256 × 256 grids. The media in these models can be taken as isotropic or transversely isotropic materials with different symmetrical axes. The free sufface condition is simply taken intoaccount by adding a number of zeros to the stress components above the free surface. It is believed that there extensively exist water feled microcracks in the crust and the upper mantle, which can be aligned under the action of stress field[7]. These aligned microcracks, which can result in the shear wave splitting in the actual recordings, are a common

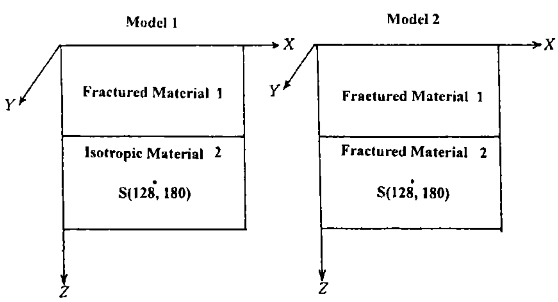

Fig. 1　Two models used for 2.5-D modeling of elastic waves in the study. The elastic constants of media are shown in Table 1 and 2. The models are discretized into 256 × 256 grids, and the spacing interval is taken as $\Delta X = \Delta Z = 0.025$ km in the case of source which is situated at the grid (128, 180), and 0.10 km in the case of plane waves which propagate vertically to the free surface. The receivesrs are put along x-axis. The symmetrical axis of water felled fractured material in both two models is perpendicular to z-axis and with an angle of 45° to x-axis.

cause of anisotropy in the crust[3]. The elastic constants of transvesely isotropic media used in the models are calculated from the corresponding isotropic media containing aligned micro fractures or cracks by using Huderson's (1981) second-order approximation theory. Two kinds of materials with water filled fractures are used in the study and we take the same elastic constant values as Lou (1995). The fracture density (CD) of 0.10, ($CD = Na^3/V$, N being the number of cracks of radius a in volume V), is used for the calculation of elastic constants of the fractured media. Table 1 shows the parameters of isotropic media, and Table 2 presents the elastic constants of frqctured media whose symmetricalaxis is parallel to the z-axis. Fig. 2 shows the velocity variation of three types of waves, longitudinal waves P, transverse waves S1 and S2. S1 and S2 have different velocities in the same direction. This is the reason of shear wave splitting in the transversely istropic media. In isotropic media, these three types of waves become purely longitudinal and purely transverse waves, corresponding to P-waves, SH-waves and SV-waves.

Fig. 3 shows the snapshots exited by SH-type source at grid (128, 180) in model 1, whose material in the upper layer is water felled fractured materia 1 with symmetrical axis perpendicular to z-axis and with an angle of 45° to x-axis and the lower half space is the isotropic material 2, is filled in the lower half space, at the time of 0.4s, whenthe waves just reach the interface, and 0.8s. In the lower layer, only U_y component is not zero. After waves progagate into the upper layer, the displacements of all three components are not equale to zero. We can see clearly the

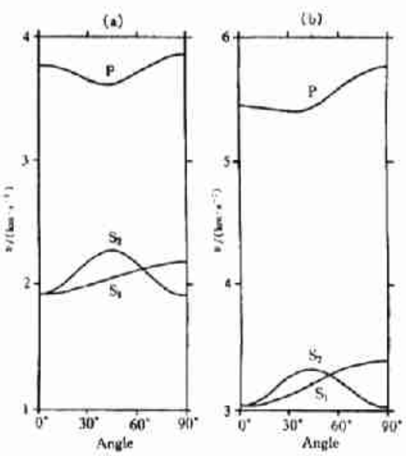

Fig. 2 The curves of phase velocity variation with respect to the angle between the phase normal of waves and the symmetrical axis of the media, for water felled fractured material 1(a) and for water filled fractured material 2(b).

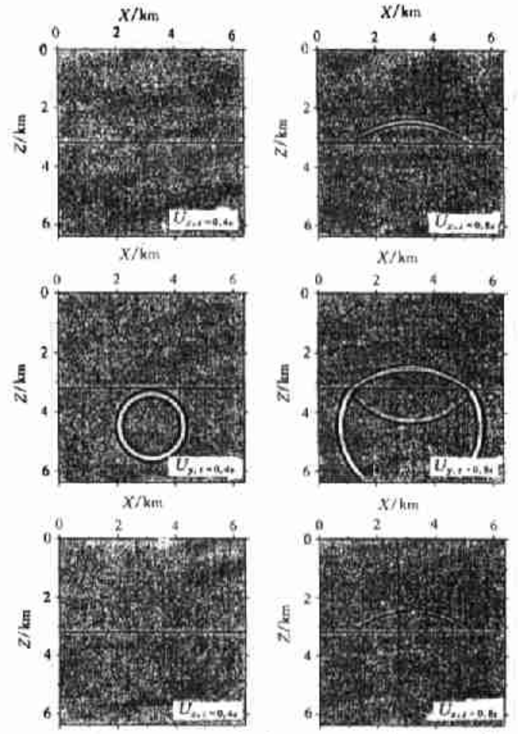

Fig. 3 The three-component displacement snapshots exited by a SH-type source at the grid (128, 180) in the model 1 of 256 × 256 grids at tme of 0.4 s, when the shear waves just reach the inter surface, and 0.8 s. The positive direction of x-axis points right and that of z-axis down. The material in the upper layer is water filled fractured material 1 with symmetrical axis perpendicular to z-axis and with an angle of 45° to x-axis. The isotropic material 2 is filled in the lower half space, in which only U_y is not equal to zero. When waves propagate into the upper layer, shear waves split apart. The weak converted P-waves also can be seen on U_x and U_z components. The absorbing condition is put at the bottom and at the both sides of the model.

splitting shear waves in th U_y component and weak converted P-waves in the U_z-component. The waves in the lower half space are purely shear waves[28]. Fig.4 is the three displacement seismograms recorded at the top of the model for this example. The two shear waves completely separate in the U_x and U_y components. There are weak P-waves arriving before the two shear waves on the U_z component. We can also see the artificial reflections from absorbing boundaries. The maximum time delay between fast and slow splitting shear waves is about 0.25 s.

Table 1 Isotropic parameters

Material	V_p /(km·s^{-1})	V_s /(km·s^{-1})	Density /(g·cm^{-3})
Material 1	4.00	2.20	2.50
Material 2	5.80	3.20	2.60

Table 2 Elastic constants for transversely isotropic media

Fractured material	A/GPa	C/GPa	F/GPa	L/GPa	N/GPa
Fractured material 1	37.290	35.500	10.480	9.130	11.830
Fractured material 2	86.444	77.037	24.091	23.911	30.056

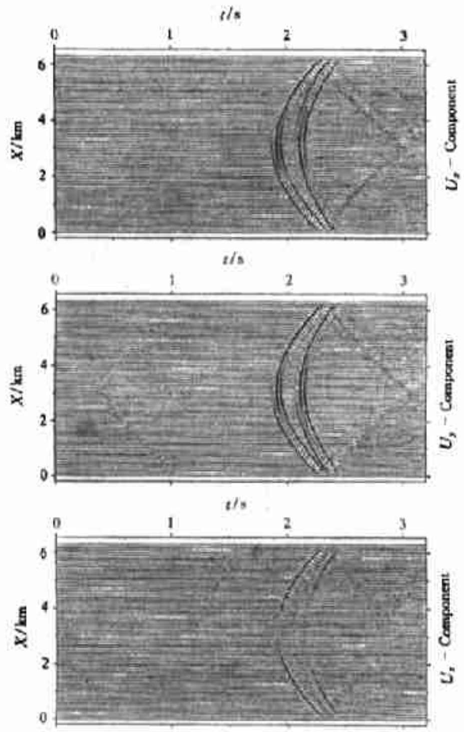

Fig.4 The three-component displacement seismograms resulted from a SH-type source at grid(128, 180)and recorded at the top of model 1. The two split shear waves can be clearly seen on the U_x and the U_y compoents. There are weak converted P-waves arriving before the shear waves on the U_x and U_z components The maximum time delay between the fast and slow shear waves is about 0.25 s. The artificial reflections from the absorbing boundaries can also be seen. In the calculation, $\Delta X = \Delta Z = 0.025$ km.

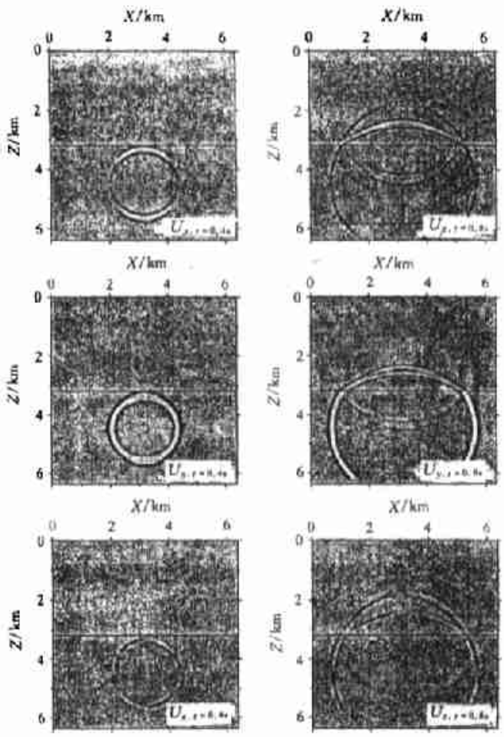

Fig.5 The three-component displacement snapshots exited by a SH-type source at the grid (128, 180)in the model 2 of 256×256 grids at time of 0.4 s and 0.8s. The positive direction of x-axis points right and that of z-axis down. The materials in the upper layer and in the lower half space are water filled fractured material 1 and 2 with a symmetrical axis perpendicular to z-axis and having an angle of 45° to x-axis. Both in the lower half space and in the upper layer, the three components are coupled together and the split shear waves can be seen. The weak P-waves are generated in the lower half space even for a SH-type source. The absorbing condition and spacing interval is the same as in model 1.

Like Fig. 3, Fig. 5 shows the snapshots exited also by SH-type force at grid (128, 180)in the model 2. The materials in the upper layer and lower half space are fractured material 1 and 2. The directions of symmetrical axes of both materials are perpendicular to the z-axis and with an angle of 45° to the x-axis. The three-component seismograms recorded at the top of the model are shown in Fig. 6. Compared with Fig. 3, Fig. 5 displays relatively complicated wave field. There also exist weak P-waves in the lower half space even for a simple SH-type source. In these two models, the space interval of grids is 25 meters, and the absorbing condition is put on the both sides and the bottom. If we rotate the U_x and the U_y components in Fig. 4 and Fig. 6 into the directions perpendicular and parallel to the symmetrical axis of the media, we can find that the direct fast shear waves only appear on the components whose polarization is perpendicular to the symmetrical axis.

Fig. 7 shows the three displacement components (U_x, U_y and U_z) of Gaussian plane waves S_1, which propagate vertically upward in the model 2 mentioned above. The spacing interval of 100 meters is used in this callculation. Receivers are also at the top of the model. Absorbing

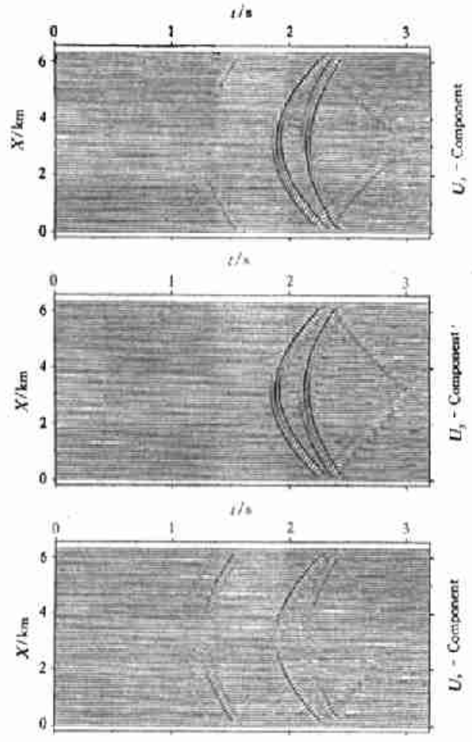

Fig. 6 The three-component displacement seismograms resulted from a SH-type source at grid (128, 180) and recorded at the top of model 2. The tow split shear waves can be clearly seen on the U_x and the U_y components. There are weak direct and converted P-waves arriving before the shear waves on the U_x and U_z components. The maximum time delay between the fast and slow shear waves is larger than that in Fig. 3. The artificial reflections from the absorbing boundaries can also be seen. Other parameters are the same as those in model 1.

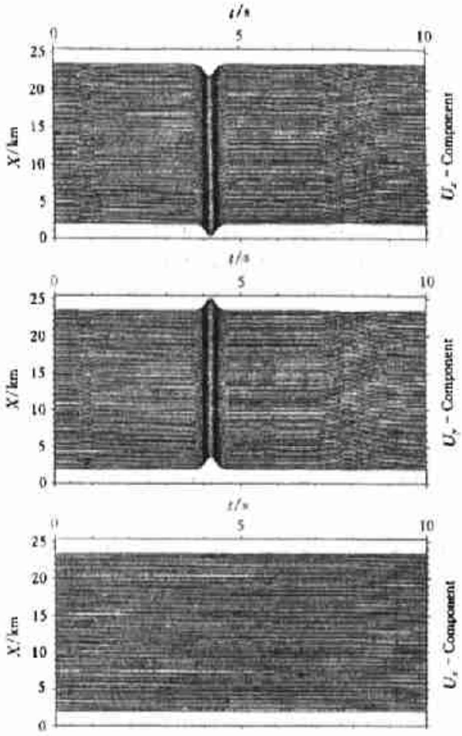

Fig. 7 The three-component displacement seismograms resulted from a Gaussian type plane waves S_1, which propagate vertically in the model 2 mentioned in the Fig. 5. The receivers are put at the free surface. The absorbing condition is only imposed at the bottom of the model. The Z-components equal zero, which means that the polarization direction of plane shear waves S_1 is perpendicular to the z-axis. Actually, it is perpendicular to the symmetrical axis and the direction of wave propagation. The spacing interval, $\Delta X = \Delta Z = 0.10$ km, is taken in the calculations.

condition is only put at the bottom of the model. We can see that both U_x and U_y do not equal zero, whereas U_z equals zero, which means that the polarization direction of plane S_1 waves is perpendicular to the z-axis. Actually, in this case, the polarization of S_1 is perpendicular to both the symmetrical axis and the direction of wave propagation.

7 Conclusion and Discussion

We have developed a pseudo-spectral method to simulate wave propagation in transversely isotropic heterogeneous media. This method can be used to calculate wave field not only exited by a source but also caused by plane wave incidence in heterogeneous transversely isotropic media with arbitrary directions of symmetricalaxes. The results of simulation show that this method is able to calculate synthetic seismograms and wave-fields in the media with free surface and with different materials such as isotropic or transversely isotropic media (water filled fractured media). This method is a very useful tool to help seismologists and geophysicists understand and interpret the wave propagation in complicated media such as inhomogeneous anisotropic media.

REFERENCES

[1] Bamford D. Pn velocity anisotropy in a continental upper mantle[J]. Geophs. J. R. astr. Soc., 1977, 49: 29～48.

[2] Makeeva L I, Plesinger A, Horalek J. Azimuthal anisotropy beneath the Bohemian massif from broad-band seismograms of SKS waves[J], Phys. Earth Planet. Int., 1990, 62: 298～306.

[3] Crampin S, Lovell J. A decade if shear wave splitting in the earth's crust: what does it mean? what use can we make of it? and what should we do next? [J]. Geophys. J. Int., 1991, 107: 387～407.

[4] Xiaodong Song, Paul G Richards. Seismological evidence for differential rotation of the earth's inner core[J]. Nature, 1996, 382: 221～224.

[5] Bennett A M. Inner core rotation rate from small-scale heterogeneity and time-varying travel times[J]. Science, 1997, 278: 1284～1288.

[6] Crampin S, Booth D C. Shear wave polarization near the north /Analia fault, II, Interpretation in terms of crack-induced anisotropy[J]. Geophys. J. R. astr. Soc., 1985, 83: 75～92.

[7] Hudson J A. Wave speeds and attenuation of elastic waves in material containing cracks[J]. Geophys, J. R. astr. Soc., 1981, 64: 133～150.

[8] Babuska V, Cara M. Seismic anisotropy in the earth[M]. Kluwer Academic, the Netherlands, 1991.

[9] Takenaka H. Modeling seismic wave propagation in complex media[J]. J. Phys. Earth, 1995, 43: 351～368.

[10] Min Lou, Rial J A. Modelling elastic-wave propagation in inhomogeneous anisotropic media by the pseudo-spectral method [J]. Geophys. J. Int. 1995, 120: 60～72.

[11] Furumura T, Takenaka H. 2.5-D modelling of elastic waves using the psudospectral method[J]. Geophys. J. Int., 1996, 124: 820～832.

[12] Furumura T, Kennett B L N, Takenaka H. Parallel 3-D psudospectral simulation of seismic wave propagation[J]. Geophysics, 1988, 63: 279～288.

[13] Shu-Huei Hung, Donald W Forsyth. Modelling anisotropic wave propagation in oceanic inhomogeneous structures using the parallel multidomain pseudo-spectral method[J]. Geophys. J. Int., 1998, 133: 726～740.

[14] Chapman C H, Drummond R. Body-wave seismograms in inhomogeneous media using Maslov asymptotic theory[J]. Bull. Seis. Soc. Am., 1982, 72: S227～S317.

[15] Alterman Z, Karal F C Jr. Propagation of elastic waves in layered media by finite difference methods[J], Bull. Seis. Soc. Am., 1968, 58: 367～398.

[16] Kelly K R, Ward R W, Sven Treitel, Alford R M. Synthetic seismograms: a finite difference approach[J]. Geophysics, 1976, 41: 2～27.

[17] Virieux J. P-SV wave propagation in heterogeneous media: velocity stress finite-difference method[J]. Geophysics, 1986, 51: 889～901.

[18] Smith W D. The application of finite element analysis to body wave proaagation problems[J]. Geophys. J. R. astr. Soc., 1976, 42: 747～768.

[19] Kosloff D, Baysal E. Forward modeling by a Fourier method[J]. Geophysics, 1980, 47: 1402～1412.

[20] Kosloff D, Reshef M, Loewenthal D. Elastic wave calculations by the Fourier method[J]. Bull. seis. Soc. Am., 1984, 74: 875～891.

[21] Fornberg J. The pseudo-spectral method: comparisons with finite differences for the elastic wave equation[J]. Geophysics, 1987, 52: 483～501.

[22] Reshef M, Kosloff D, Edwards M, HsingC. Three-dimension acoustic modelling by the Fourier method[J]. Geophysics, 1988a, 53: 1175～1183.

[23] Reshef M, Kosloff D, Edwards M, Hsing C. Three-dimension acoustic modelling by the Fourier method[J]. Geophysics, 1988b, 53: 1184～1193.

[24] Gazdag J. Modeling of the acoustic wave equation with transform methods[J]. Geophysics, 1981, 46: 854～859.

[25] Daudt C R, Braile L W, Nowack R L, Chiang C S. A comparison of finite-difference and Fourier method calculations of synthetic seismograms[J]. Bull. seis. Soc. am., 1989, 79: 1210～1230.

[26] Cerjan C, Kosloff D, Kosloff R, Reshef M. A nonreflecting boundary condition for discrete acoustic and elastic equations[J]. Geophysics, 1985, 50: 705～708.

[27] Fedorov F I. The theory of elastic waves in crystals[M]. Plenum Press, New York, 1968.

[28] Adi K, Richards P G. Quantitative seismology: theory and methods[M]. Freeman, San Francisco, 1980.

利用伪谱法模拟横向各向同性介质中的波*

张范民[1]，竹中博士[2]，李清河[1]，王彦宾[2]

(1. 中国地震局兰州地震研究所，甘肃 兰州 730000；

2. 日本九州大学理学部地球行星科学系，福冈 812-81)

摘要：介质的弹性常数为三维四阶张量的分量，共有 81 个. 由于应力张量和应变张量的对称性及能量密度是应变的二次函数，一般各向异常性介质的独立弹性常数可减为 21 个. 如果介质具有较高的对称性，独立弹性常数的数目会更少.

对于地壳和上地幔，具有 5 个独立弹性常数的横向各向同性介质是一个非常好的近似. 本研究中横向各向同性介质的对称轴方向可以是任意的(即对称轴可以不平等于铅直方向)，在此情况下，需要进行坐标变换. 如果已知介质在某一坐标系(其坐标轴平行或垂直于介质的对称轴)中的弹性常数，我们能够容易地利用变换公式得到变换后新坐标系中的弹性常数.

本文提出了一种方案，利用伪谱法既能模拟横向各向同性介质中的平面波，也能模拟点源激发的波场. 在勘探地球物理和地震学中，模拟横向各向同性介拮中传播的平面波及区域源产生的波是最重要的研究课题之一. 然而在一般各向异性介质中，很难或不可能确定弹性波的相速度和偏振方向，但在横向各向同性介质中，则可以通过坐标变换来实现. 这里我们所提出的方法可以用于横向各向同性介质中弹性波的模拟.

主题词：数字模拟；地震波；各向异性；横向各向同性；伪谱法

中图分类号：P315.3；P315.8 **文献标识码**：A **文章编号**：1000-0844(1999)02-0214-11

收稿日期：1998-10-07

* 中国地震局兰州地震研究所论著编号：LC1999017

第一作者简介：张范民，男，1963 年 9 月生，副研究员，从事地震波理论与应用研究.